Korean J. Chem. Eng., 34(5), 1358-1365 (2017)
DOI: 10.1007/s11814-017-0027-z

pISSN: 0256-1115
eISSN: 1975-7220

Enhanced ketalization activity of cyclohexanone and ethanediol over immobilized ionic liquid in mesoporous materials

Liming Dai, Qian Zhao, Haibo Zhao, Yingying Li, and Tingshun Jiang†

School of Chemistry and Chemical Engineering, Jiangsu University, Zhenjiang 212013, Jiangsu, China
(*Received 21 November 2016 • accepted 6 February 2017*)

Abstract−Three different mesoporous molecular sieves, including MCM-41, MCM-48, and SBA-15, were synthesized by hydrothermal process and characterized by XRD, BET and TEM. The chlorine-aluminate acidic ionic liquid of 1-butyl-3-methylimidazolium chloride-aluminum chloride ([Bmim]Cl-$AlCl_3$, denoted as Al-ILs) was prepared by two-step method. The immobilized ionic liquid (SBA-15/Al-ILs, MCM-41/Al-ILs, MCM-48/Al-ILs) was prepared through impregnating Al-ILs. The structures of composite catalysts were characterized by XRD, BET, FT-IR, TEM and XPS. The amounts of aluminum present in the resulting composite catalysts were detected by ICP-AES to calculate the amount of AL-ILs impregnated. The ketalization between cyclohexanone and ethanediol was used as the model reaction to test the catalytic activities of the composite catalysts. The effects of molar ratio of the reactants, reaction time, the catalyst dose, as well as the addition of cyclohexane were discussed in detail. Also, catalytic activities of three catalysts with different pore sizes were compared. Under comparable conditions, the SBA-15/Al-ILs composite catalyst exhibited much high catalytic activity and gave a maximum yield that was *ca.* 85.1%.

Keywords: Ionic Liquid, Immobilization, Mesoporous Molecular Sieve, Impregnation, Ketalation

INTRODUCTION

Ionic liquids, as environmental solvent or catalyst, have gained a great deal of attention owing to their excellent properties such as low vapor pressure, non-flammability, and wide electrochemical window [1-3]. On the other hand, ionic liquid, completely composed of ions, can be designed to possess a definite set of properties. Therefore, ionic liquids have a substantial potential in catalysis [4,5]. Huang et al. applied different ionic liquids as the catalyst for the reaction of oxidation of 1, 3-diisopropylbenzene and found that [C_4mim]OH was very suitable for that reaction [6]. Qiu et al. employed four novel Brønsted acidic ionic liquids to synthesize biodiesel from coconut oil and obtained a high yield [7]. Xu et al. employed a tetramethylammonium-based amino acid ionic liquid to synthesize benzaldehyde from cinnamaldehyde and obtained a high yield [8]. Nevertheless, as catalyst, ionic liquids have some restrictions which have been reported by several authors [9,10]: (1) the viscosity of ionic liquid vastly affects the mass and heat transfer rate, (2) liquid catalyst is hard to recycle and separate from the product, and (3) its high price makes it hard to industrialize.

Mesoporous molecular sieve is a type of material with large specific surface area [11]. The concept of immobilized ionic liquids on the mesoporous molecular sieve would expand the scope of application of ionic liquids and strengthen the capacity of mass and heat transfer of catalyst, which exhibit more outstanding performance of the material [12]. The composite catalyst, converting the homogeneous to the heterogeneous, which would greatly reduce waste and pollution, is consistent with the requirements of green chemistry [13]. He et al. immobilized the porcine pancreatic lipase on the SBA-15, which was modified by the carboxylation ionic liquid through both physical absorption and chemical bond. And it was demonstrated very suitable for the hydrolysis of acetoglyceride [14]. Lee et al. proved that the silica-supported 1-propyl-3-n-butylimidazolium bromide is an effective heterogeneous catalyst for synthesis of cyclic carbonate from allyl glycidyl ether (AGE) and carbon dioxide [15]. Chen et al. used the mesoporous SiO_2 modified by ionic liquid to support the LaW_{10} and applied it to deep desulfurization [16].

Ketalation, a class of spices, is commonly used in the synthesis of carbohydrate, and as the protection of carbonyl composite, or the target production of intermediates of paint, food, tobacco, cosmetics and pharmaceutical industries [17-19]. Traditional acid catalysts, inorganic acid, inorganic acid salt or p-toluene sulfonic acid etc., are not entirely satisfactory owing to the problem of corrosion, tedious workup, and environmental polluting [20]. Consequently, there is a demand for new acid catalysts to synthesize ketalation. For example, Rabindran applied Al-MCM-41 as the acidic catalyst for the ketalation between cyclohexanone and ethanediol with 75.1% yield [18]. The chlorine-aluminate acidic ionic liquids is a type of ionic liquid prepared by mixing metal halide and organic halide, and has been used as a Lewis acid catalyst for many reactions [21]. Moreover, the ratio of aluminum chloride to organic bases greatly affects the Lewis acidity of ionic liquids through the anion equilibrium (chloride is an example) expressed as follows [22]:

$$AlCl_3 + Cl^- \longrightarrow AlCl_4^-$$
$$2AlCl_4^- \rightleftharpoons Al_2Cl_7^- + Cl^-$$

The more the metal halide is, the stronger acidic the ionic liq-

†To whom correspondence should be addressed.
E-mail: tshjiang@ujs.edu.cn

uid will be, when the fraction of metal halide is more than 0.5 [23]. Hence, the ionic liquid has the potential to catalyze ketalation. However, in comparison to the concentrated sulfuric acid and hydrofluoric acid, ionic liquid has higher cost and more complex process. Meanwhile, liquid catalyst would increase the post-treatment process, restricting the application of acidic ionic liquids. When immobilized acidic ionic liquid on the mesoporous molecular sieve, it would combine the special open-framework structure of mesoporous molecular sieve and the catalytic active of acidic ionic liquids, which have a potential advantage in solid acid catalyst.

In the present work, the immobilized chlorine-aluminate acidic ionic liquid was the first applied to the ketalization between cyclohexanone and ethanediol. And taking into account of influence of pore structure, different mesoporous molecular sieve was synthesized to loading ionic liquid. The structure and surface property of immobilized ionic liquid was studied. The effects of reactant molar ratio, catalyst dose, reaction time and the usage of cyclohexane on the yield of ketalization were also investigated in detail. The composite catalyst proved to be very good for the reaction of the ketalation between cyclohexanone and ethanediol.

EXPERIMENTAL

1. Material

The poly (ethylene glycol)-block-poly (propylene glycol)-block-poly (ethylene glycol) (Pluronic P123), used as the structure-directing agent in SBA-15 synthesis process, was purchased from Aldrich Company. The 1-methylimidazole (>99%), 1-chlorobutane (>99%), anhydrous aluminium chloride, tetraethoxy silane (TEOS), cetyl trimethyl ammonium bromide (CTAB), NaOH, NaF, sodium metasilicate nonahydrate, sulfuric acid (98 wt%), hydrochloric acid (37 wt%), anhydrous ether, chloroform, and dichloromethane, used in the experiment, were analytical grade and were purchased from Shanghai Chemical Reagent Corporation, China.

2. Synthesis of MCM-48

MCM-48 mesoporous molecular sieves were synthesized according to a molar ratio of 1 TEOS: 0.65 CTAB: 0.5 NaOH: 0.1 NaF: 62 H_2O [24]. A typical synthesis process was as follows: 0.9 g of NaOH and 10.62 g of CTAB were dissolved in 50 ml distilled water and the mixture was gently stirred at 35 °C for 30 min. Then, 10 ml of TEOS and 0.19 g of NaF were slowly added into the above mixture. After continued stirring for another 1 h at 35 °C, the resulting solution was transferred to a 100 ml Teflon-lined autoclave and crystallized at 100 °C for 24 h in an oven. After cooling to room temperature, the sample was washed with distilled water, and dried at 50-60 °C for 24 h to obtain a dried sample. The dried sample was heated to 550 °C at a heating rate of 2 °C/min and calcined at 550 °C in air for 6 h to remove the template.

3. Synthesis of MCM-41

MCM-41 mesoporous molecular sieve was hydrothermally synthesized as the following process: 28.42 g of sodium metasilicate nonahydrate was dissolved in 40 ml of distilled water and the mixture was stirred at 35 °C in the boiling flask-three-neck until solid was thoroughly dissolved. 7.289 g of CTAB was dissolved in 40 ml of distilled water to form transparent solution and was slowly added into the above solution. After continued stirring at 35 °C for 0.5 h, the pH of the mixed solution was adjusted to 11 by dropwise addition of sulfuric acid (50 vol%). After stirring for 3 h, the resulting solution was transferred into a 100 ml Teflon-lined autoclave and crystallized at 120 °C for 24 h in an oven. After cooling to room temperature, the sample was washed with distilled water to neutral, and dried at 50-60 °C for 24 h to obtain a dried sample. The dried sample was heated to 550 °C at a heating rate of 2 °C/min and calcined at 550 °C in air for 6 h to remove the template.

4. Synthesis of SBA-15

SBA-15 mesoporous molecular sieve was hydrothermally synthesized according to as follows: 4.0 g of P123 and 20 mL of HCl (37 wt%) were dissolved in 120 mL of distilled water to form a transparent solution. Then, 9 mL of TEOS was added to the above solution. After stirring at 35 °C for 24 h, the mixture was aged under static condition and constant pressure at 100 °C for 48 h. After cooling to ambient temperature, the solid product was filtered, washed with distilled water, dried overnight in an oven. The dried sample was heated to 550 °C at a heating rate of 2 °C/min and calcined at 550 °C in air for 6 h to remove the template.

5. Synthesis of [Bmim]Cl-$AlCl_3$ and Immobilization Process

The syntheses of the [Bmim]Cl and the Al-ILs were according to the literature [25]. A typical synthesis procedure of the [Bmim]Cl was as follows: a certain amount of N-methylimidazolium and a slight molar excess of 1-chlorobutan were placed to the three-necked flask under nitrogen atmosphere with stirring at 80-85 °C for 48 h. After cooling to room temperature, the resulting liquid was washed by anhydrous ether three times. Then, it was transferred to vacuum drying oven at 80 °C for 12 h.

The Al-ILs was prepared by slowly adding the desired $AlCl_3$ to the imidazolium salt of [Bmim]Cl at room temperature. The reaction was left stirring for 12 h under nitrogen atmosphere and n-heptane was used as protection fluid. After that, the below liquid Al-ILs was extracted. Of which, the molar ratios of $AlCl_3$ with 1-butyl-3-methylimidazolium chloride is 2.3, and the molar content of $AlCl_3$ were calculated by the equation below:

$$X_{AlCl_3} = \frac{n_{AlCl_3}}{n_{AlCl_3} + n_{[bmim]Cl}}$$

According to this formula, X_{AlCl_3} is 0.7.

The immobilized process was conducted by direct immersion. A typical process was as follows: 5 g of Al-ILs and 5 g of mesoporous molecular sieve were added to the three-necked flask under nitrogen atmosphere, and 30 ml of chloroform was also added to the three-necked flask as the dispersant. After stirring for 12 h at room temperature, the chloroform would be evaporated. The resulting solid was extracted by soxhlet extractor with dichloromethane for 12 h. Then, it was transferred to vacuum drying oven and was dried at 60 °C for 12 h. The composite catalysts with arious ionic liquid contens were obtained and the weight ratio of Al-ILs with carriers is, respectively, 1, 2, 3 and 4, before extraction.

6. Characterization

FT-IR spectra were recorded on the Nexus FT-IR 470 spectrometer made by Nicolet Corporation (USA) with KBr pellet technique in the frequency range of 4,000-400 cm^{-1}. The surface areas and pore sizes of samples were measured by using NOVA2000e analytical system made by Quantachrome Corporation (USA). The surface

areas were calculated by Brunauer-Emmett-Teller (BET) method and pore sizes were calculated by Barrett-Joyner-Halenda (BJH) method. The powder X-ray diffraction (XRD) was performed with a Rigaku D/MAX 2500PC instrument using Cu Kα radiation (λ= 0.15418 nm), operated at 40 kV, 50 mA, a scan step of 0.02° from 0.5° to 5° (2θ) at a speed of 1°/min. Transmission electron microscopy (TEM) microphotographs were carried out on a Philips TEMCNAI-12 with an acceleration voltage of 120 kV. X-ray photoelectron spectroscopy (XPS) measurement was recorded on an ESCALAB 250 (Thermal Electron Corp.) spectrometer equipped with Al Kα X-ray source, operating at 150 W. The binding energies were referenced to the C1s binding energy at 284.8 eV. The amounts of Al in sample were determined by inductive coupled plasma (ICP) technique (Vista-MPX, Australia), and the detector was MPX CCD.

7. Ketalation between Cyclohexanone and Ethanediol

The reaction was performed at a three-necked flask equipped with a magnetic stirrer, a refluxing condenser tube and a water segregator. The desired amounts of reactants including cyclohexanone and ethanediol, the water-carrying agent of cyclohexane, as well as the compound catalyst were added to three-necked flask. The reactor was heated to 120-125 °C for a period by oil bath and then cooled to room temperature. The resulting solution was washed successively with distilled water until a neutral solution was obtained. The washed solution was placed into a separating funnel to obtain the organic phase. The organic phase then was dried by anhydrous magnesium sulfate. Under atmospheric pressure, the fraction in the range of 170-180 °C was collected as product. The above obtained product was characterized by FT-IR and refractometer, and the yield (%) of the product was calculated as follow:

$$\text{Yield}\,(\%) = \frac{\text{actual quality of product}}{\text{theoretic quality of product}} \times 100\%$$

RESULTS AND DISCUSSION

The N_2 adsorption-desorption isotherms of all samples are shown in Fig. 1. As shown in Fig. 1, the isotherms of the three carriers

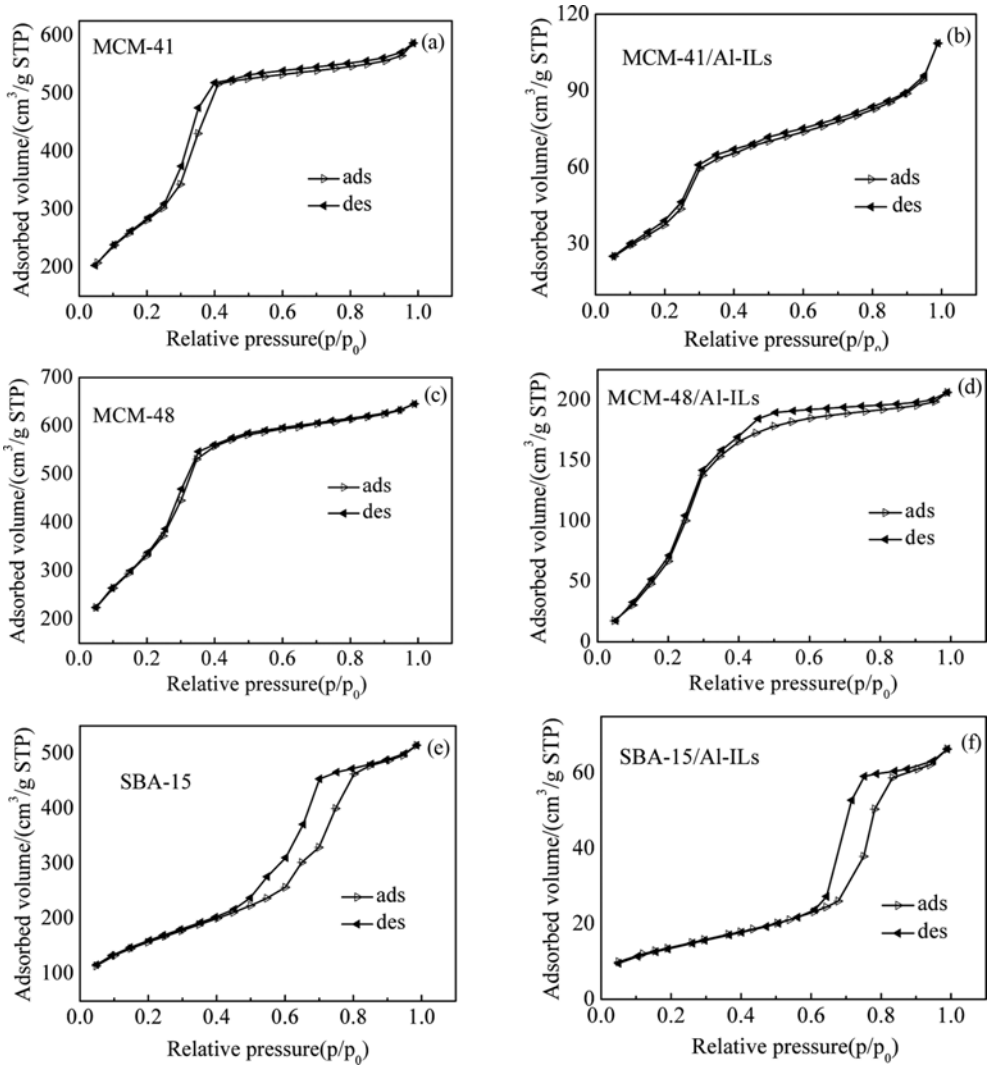

Fig. 1. N_2 adsorption-desorption isotherms of all samples.

Table 1. The BET analysis of carriers and composite catalysts

Materials	Surface area (m^2/g)	Average pore size (nm)
SBA-15	610.0	5.5
SBA-15/Al-ILs	31.2	4.9
MCM-41	1064.7	3.0
MCM-41/Al-ILs	183.2	2.8
MCM-48	1405.0	2.4
MCM-48/Al-ILs	312.6	2.1

including MCM-41, MCM-48 and SBA-15 are of the typical type IV isotherms with a hysteresis loop as defined by IUPAC, which is a characteristic of typical mesoporous materials [26,27]. While the isotherms of the three composites suggested the loss of mesoporous structure to some extent, may be owing to the introduction of ionic liquid in the synthesis of the three composites leading to the deterioration of the framework of the resulting composites. Furthermore, the corresponding textural properties are summarized in Table 1, including the BET surface areas and average pore sizes of all samples. As listed in Table 1, the specific surface areas and pore sizes of three carriers, SBA-15, MCM-41 and MCM-48 mesoporous molecular sieves, are 610, 1,064.7, 1,405 m^2/g and 5.5, 3.0, 2.4 nm, respectively. As compared with the corresponding carrier, the specific surface area of the composite catalyst obtained after loading ionic liquid decreased greatly and the average pore size also decreased. This may be explained by the reason that the pore of the carrier was occupied by the ionic liquid.

1. XPS Analysis

Fig. 2 displays the XPS spectrum of the SBA-15/Al-ILs sample. It shows that the surface of sample consisted of O, Si, C, N, and Al elements. N and Al elements mainly came from the immobilized Al-ILs. And the C may be due to the immobilized Al-ILs and the C absorbed in the air. O and Si elements were primarily attributed to the -Si-O- in the composite catalyst. Furthermore, Fig. 3 shows the XPS O1s high resolution spectrum of the SBA-15/Al-ILs with deconvolution peaks, which shows four components for O1s spectrum. And the binding energy (531.15 eV) is similar to the $Al_4Si_4O_{10}(OH)_8$ (531.17 eV), which indicates that Al-ILs has been successfully combined with SBA-15 through the covalent bonding between the aluminum atom and the Si-OH group [28], suggesting that the Si-OH functional group played an important role in the immobilized process (Physical adsorption may also exists in this typical immobilization for the reason that the surface area decreased greatly).

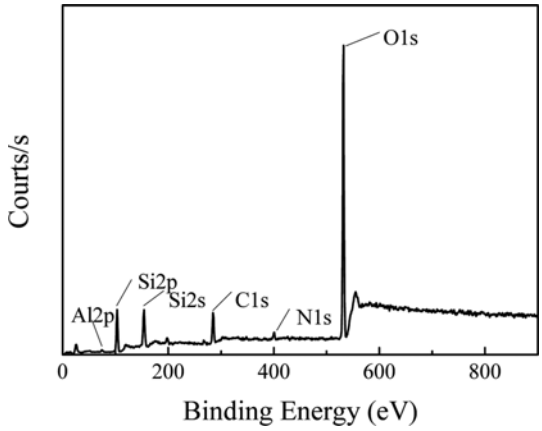

Fig. 2. XPS spectrum of the SBA-15/Al-ILs sample.

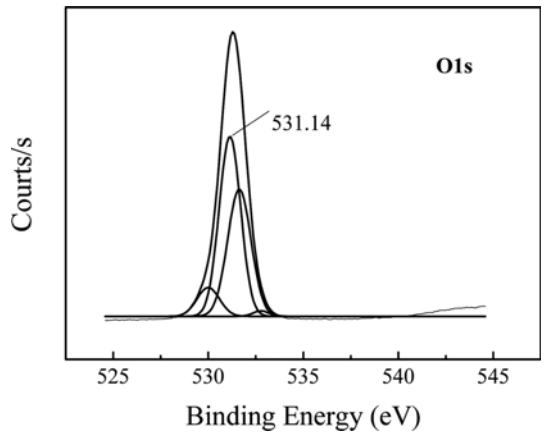

Fig. 3. XPS O1s high resolution spectrum of SBA-15/Al-ILs sample.

2. FT-IR Analysis of the Al-ILs, SBA-15/Al-ILs, MCM-41/Al-ILs and MCM-48/Al-ILs

The FT-IR spectra of Al-ILs and different composite catalysts are presented in the Fig. 4. The peaks of 2,875 cm^{-1} and 2,961 cm^{-1} in Al-ILs are characteristic of the C-H stretching vibration of straight-chain paraffin. And its flexural vibration was observed at 1,383 cm^{-1} and 1,466 cm^{-1}. The peak of 3,090 cm^{-1} is characteristic of the C-H stretching vibration of imidazole ring, and the peak of 3,416 cm^{-1} was attributed to water absorbed in ionic liquid. The adsorption bands at 1,637 cm^{-1} and 1,571 cm^{-1} were aroused by C=C and C=N bonds. Also, the above peaks were observed in the FT-IR spectra of several composite catalysts, suggesting that the Al-ILs was successfully attached to carriers. Besides these, the broad band located at 3,354 cm^{-1} for the composite catalysts was from the Si-OH and adsorbed water. While the strong peak at 1,079 cm^{-1} is assigned to the Si-O [29,30].

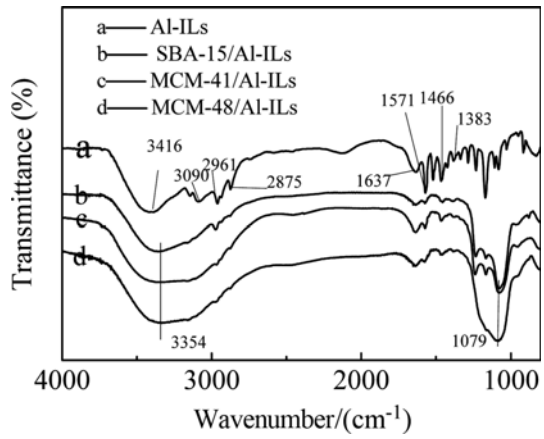

Fig. 4. FT-IR spectra of Al-ILs, SBA-15/Al-ILs, MCM-41/Al-ILs, and MCM-48/Al-ILs samples.

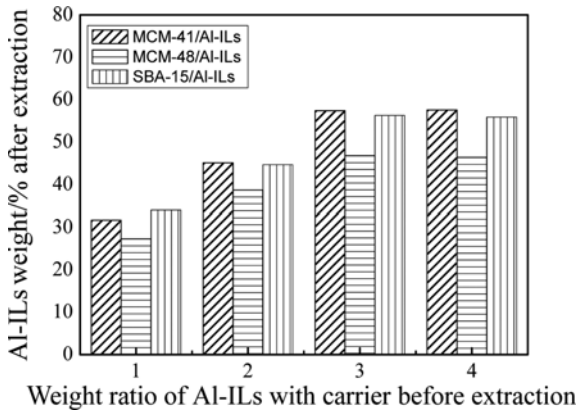

Fig. 5. Histogram of weight percentage of Al-ILs in different composite catalysts.

3. Elemental Analysis of Composite Catalysts

The aluminum amounts incorporated in framework of the composite catalysts were determined by ICP-AES, and the amount of Al-ILs in the catalyst was calculated from this value.

Fig. 5. presents the content of Al-ILs in three composite catalysts. As shown in Fig. 5, we found that with the increase of weight ratio of Al-ILs with carriers from 1 to 3, the content of Al-ILs in all composite catalysts increased. When the weight ratio reached 4, the content of Al-ILs slightly changed. This may be attributed to the fact that the capacity of each carrier was related to its surface area. The content of Al-ILs in different composite catalysts is listed in Table 2. Combined with Table 1, we found that MCM-48 had the minimum pore size and maximum specific surface area among the three carriers. From Table 2, the MCM-48/Al-ILs has the least content of Al-ILs. Therefore, we concluded that the pore size may be an important factor in immobilized process.

4. XRD Analysis

The XRD patterns of all samples are displayed in Fig. 6. As shown in Fig. 6(a), the SBA-15 sample has the diffraction peaks at *ca.* 0.9°, 1.51°, and 1.75° indexed to (100), (110) and (200), respectively. This suggests the formation of a typically ordered 2D hexagonal mesoporous structure [26]. Further, the SBA-15/Al-ILs sample also exhibited three diffraction peaks located at the same position as compared with the SBA-15 sample, and the intensities of these diffraction peaks were weak. This indicated that the SBA-15/Al-ILs sample has obvious mesoporous structure, but the mesoporous ordering decreased. As displayed in Fig. 6(b), the MCM-41 sample has a strong diffraction peak (100) at 2θ=2.3°, and has small and weak diffraction peaks (110 and 200) at 2θ=4-6°, indicating

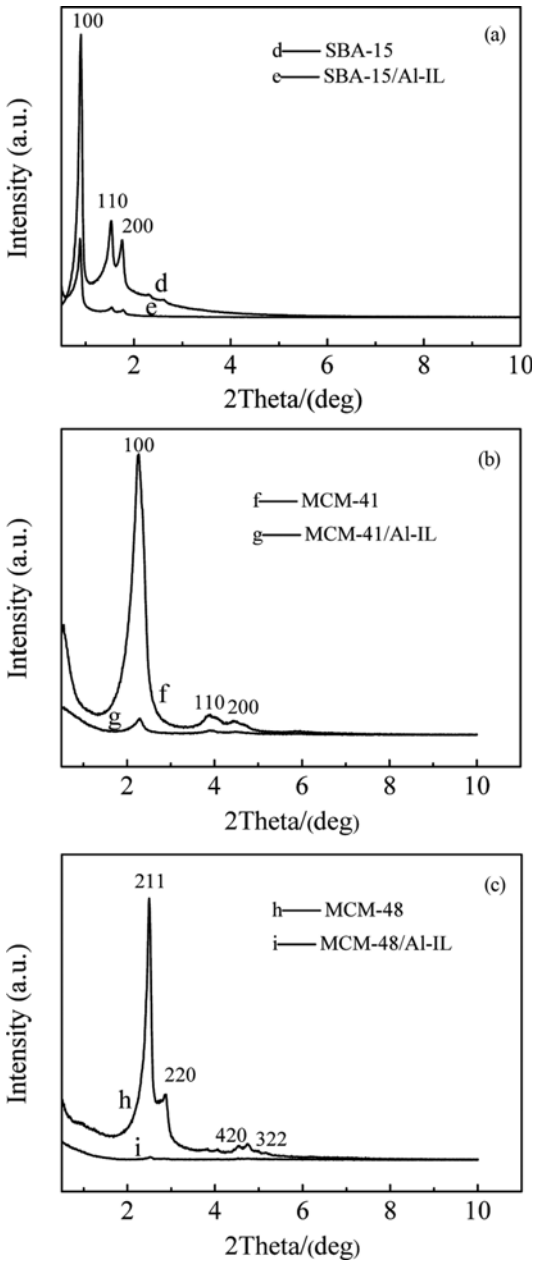

Fig. 6. XRD patterns of the composite catalysts and the carriers (a) SBA-15 and SBA-15/Al-ILs; (b) MCM-41 and MCM-41/Al-ILs; (c) MCM-48 and MCM-48/Al-ILs.

the formation of the typical hexagonal mesoporous structure of MCM-41 [27]. At the same time, after the introduction of Al-ILs,

Table 2. The contents of Al-ILs in different composite catalysts

Weight ratio of Al-ILs with carrier before extraction	MCM-41/Al-ILs (Al-ILs wt%) after extraction	MCM-48/Al-ILs (Al-ILs wt%) after extraction	SBA-15/Al-ILs (Al-ILs wt%) after extraction
1 : 1	31.7	27.3	34.0
2 : 1	45.1	38.7	44.7
3 : 1	57.4	46.8	56.3
4 : 1	57.6	46.4	55.9

the resulting MCM-41/Al-ILs sample only had a weak diffraction peak (100), and the other diffraction peaks disappeared, suggesting that the introduction of Al-ILs resulted in a certain extent damage of the mesoporous structure of MCM-41. According to Fig. 6(c), hat the MCM-48 sample exhibited four diffraction peaks, located at 2θ=2.51, 2.86, 4.53 and 4.76° that can be indexed to (211), (220), (420) and (322), showing the formation of a typical *Ia3d* cubic mesoporous framework with long range ordering [31]. However, the mesoporous framework of the MCM-48/Al-ILs sample was destroyed when a certain content of Al-ILs was introduced in MCM-48 sample. Therefore, we can conclude that the mesoporous structure of SBA-15/Al-ILs sample was well reserved as compared to the MCM-41/Al-ILs and MCM-48/Al-ILs samples, which was probably due to the good hydrothermal stability of SBA-15 [32,33].

5. TEM Analysis

The TEM images of all samples are shown in Fig. 7. In Fig. 7(a), c and e, all carriers exhibit clear pores and pore channels, suggesting the formation of ordered mesoporous framework. At the same time, from Fig. 7(b), d and f after ionic liquid was immobilized, the SBA-15/Al-ILs still had obvious mesoporous structure, but the mesoporous ordering decreased as compared with the SBA-15. While the mesoporous structure of the MCM-41/Al-ILs was to a certain degree damaged. For the MCM-48/Al-ILs sample, the mesoporous structure almost disappeared. This is consistent with the results of XRD ananlysis.

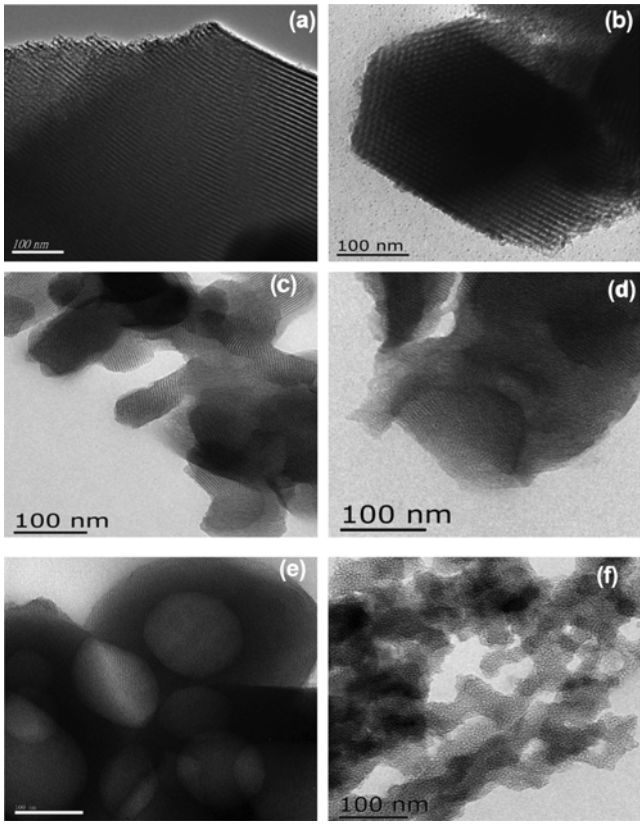

Fig. 7. TEM images of all samples (a) SBA-15; (b) SBA-15/Al-ILs; (c) MCM-41; (d) MCM-41/Al-ILs; (e) MCM-48; (f) MCM-48/Al-ILs.

Table 3. Catalytic activity of composite catalysts with different carriers

Catalyst	Yields (%)
SBA-15	No product
MCM-41	No product
MCM-48	No product
Al-ILs	86.0
SBA-15/Al-ILs	85.1
MCM-41/Al-ILs	81.4
MCM-48/Al-ILs	75.3

6. Catalytic Activity

6-1. Effect of Different Catalysts on the Yield of Product

Table 3 lists the results of ketalation of cyclohexanone and ethanediol over all composite catalysts, carriers and pure ionic liquid. In this reaction, 1.5 : 1 of the mole ratio of ethanediol with cyclohexanone (10.44 ml), 15 ml of cyclohexane and 0.5 g of catalyst dose were added into the reactor, respectively; reaction time was 75 min, reaction temperature was 120-125 °C. According to Table 3, the SBA-15/Al-ILs catalyst exhibited the highest catalytic activity among three composite catalysts and the yield of cyclohexanone ethylene ketal could reach 85.1% after reaction for 75 min, slightly less than the pure ionic liquid, while the carriers show almost no catalytic activity. From the results above, we could conclude that the SBA-15/Al-ILs catalyst is a good catalyst for synthesis of cyclohexanone ethylene ketal as compared with the other two catalysts. This may be owing to the good mesoporous framework of the SBA-15/Al-ILs, which is beneficial to the adsorption and desorption for reactants and products [34]. So, SBA-15/Al-ILs was chosen as catalyst for further test.

6-2. Effect of the Mole Ratio of Ethanediol with Cyclohexanone on the Yield of Product

Fig. 8 presents the results of the effect of the mole ratio of ethanediol with cyclohexanone on the yield of cyclohexanone ethylene ketal using SBA-15/Al-ILs as catalyst. As shown in Fig. 8, the yield of cyclohexanone ethylene ketal increased with increase of

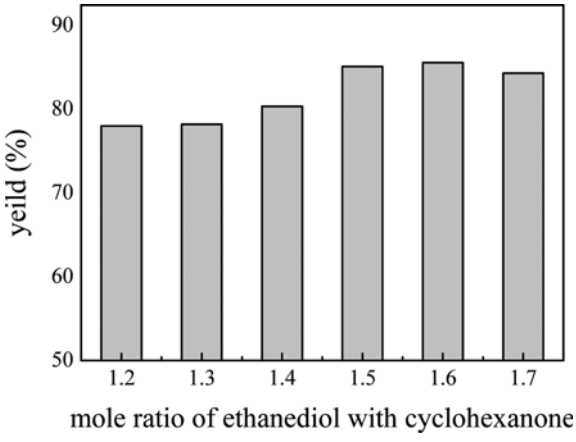

Fig. 8. Effect of ratio mole of ethanediol with cyclohexanone on the yield of product (catalyst dose=0.5 g, reaction time=75 min, reaction temperature 120-125 °C, cyclohexane=15 ml, cyclohexanone=10.44 ml).

the mole ratio of ethanediol with cyclohexanone from 1.2 to 1.6. When the mole ratio of ethanediol with cyclohexanone reached 1.7, the yield of cyclohexanone ethylene ketal decreased. This phenomenon may be owing to the occupancy of cyclohexanone onto the active sites and the availability of ethanediol molecules in further reaction processing [18].

6-3. Effect of the Amount of Cyclohexane on the Yield of Product

The effect of the amount of cyclohexane on the yield of product was investigated and the results shown in Fig. 9. From Fig. 9, the yield of product increased from 75.9% for the amount of cyclohexane 10 mL to 85.1% for 15 mL, and decreased to 78.9% as the amount of cyclohexane increased to 20 mL. This phenomenon may be owing to as follows: according to chemical equilibrium principle, a certain amount of cyclohexane could remove the water in a timely manner, resulting in the yield of product. On the other hand, the reactants were diluted when the amount of cyclohexane was further increased. In this case, the cyclohexanone was hard to form carbonium ion in active sites, and the ethanediol was difficult to further react with carbonium ion. 15 ml of the cyclohexane was probably the best condition.

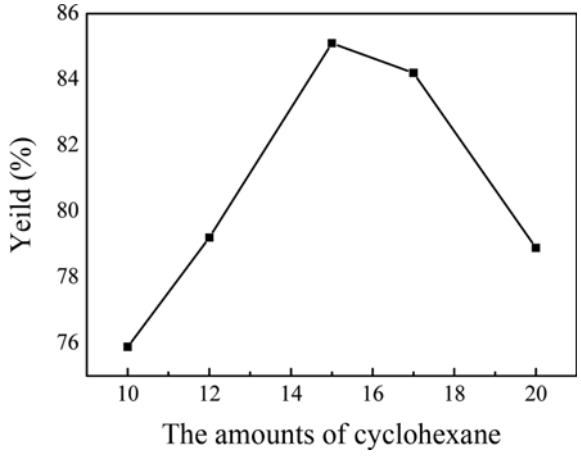

Fig. 9. Effect of the amount of cyclohexane on the yield of product (reaction time=75 min, reaction temperature=120-125 °C, mole ratio of ethanediol with cyclohexanone (10.44 mL)=1.5, catalyst dose=0.5 g).

Table 4. Effect of catalyst dose and reaction time on the yield of product

Material	Reaction time (min)	Catalyst dose (g)	Yield (%)
SBA-15/Al-ILs	30	0.5	73.87
	60	0.5	82.9
	75	0.5	85.1
	90	0.5	84.94
	120	0.5	84.98
	75	0.2	73.15
	75	0.3	76.58
	75	0.4	82.34
	75	0.5	85.1
	75	0.6	85.2

6-4. Effect of Catalyst Dose and Reaction Time on the Yield of Product

Table 4 lists the results of the effect of catalyst dose and reaction time on the yield of product over SBA-15/Al-ILs catalyst. Reaction conditions: reaction temperature was 120-125 °C, the mole ratio of ethanediol to cyclohexanone (10.44 ml) was 1.5 : 1, and addition of cyclohexane was 15 ml. As listed in Table 4, 0.5 g of catalyst and 75 min of reaction time were best condition for the ketalation between cyclohexanone and ethanediol, and the maximum yield (%) was 85.1%. The yield (%) increased immensely before 75 min, and almost had no change for the reason of the limitation of chemical equilibrium.

6-5. The Reusability of Catalyst

The reusability of SBA-15/Al-ILs catalyst was also evaluated using the ketalation between cyclohexanone and ethanediol. As shown in Fig. 10, the yield of product decreases from 85.1% to 81.3% after four times of recycling. The main reason may be that part of Al-IL in catalyst was lost during the recycling.

6-6. Composition Analysis of Ketalation between Cyclohexanone and Ethanediol

Fig. 11 illustrates the FT-IR spectrum of ketalation of cyclohex-

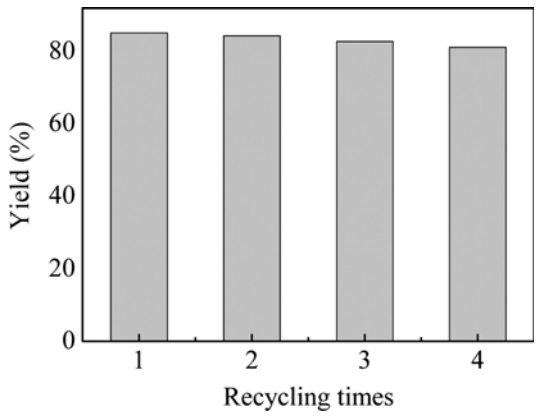

Fig. 10. Recycling of SBA-15/Al-IL in the ketalation between cyclohexanone and ethanediol (catalyst dose=0.5 g, reaction time=75 min, reaction temperature 120-125 °C, cyclohexane=15 ml, mole ratio of ethanediol with cyclohexanone (10.44 mL)=1.5).

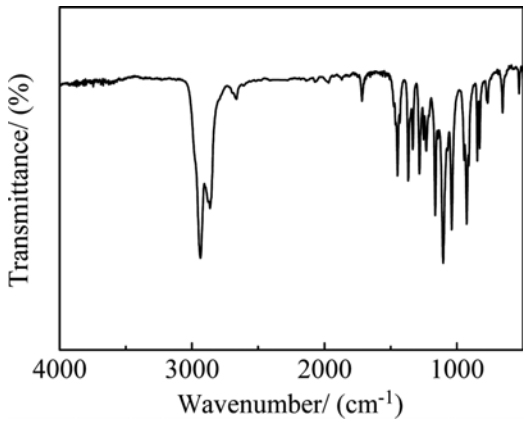

Fig. 11. FT-IR spectrum of ketalation of cyclohexanone with ethanediol using the SBA-15/Al-ILs as the catalyst.

anone with ethanediol. The adsorption bands at 2,936 cm^{-1}, 2,863 cm^{-1}, 1,447 cm^{-1}, and 767 cm^{-1} were assigned to the C-H stretching vibration or flexural vibration. The C-O-C has the characteristic bands at 1,163 cm^{-1} and 1,103 cm^{-1}. There is no the spectrum of -OH in Fig. 11 and only a weak band of C=O appears. Its refractive index n_D^{20}=1.4586 (the refractive index of the standard ketalation between cyclohexanone and ethanediol n_D^{20}=1.4583). The above results can prove that the production is ketalation between cyclohexanone and ethanediol.

CONCLUSIONS

Highly ordered mesoporous molecular sieve carriers SBA-15, MCM-48 and MCM-41, with large surface areas, were successfully synthesized by hydrothermal method and proved to be very fit for immobilizing Al-ILs. Based on TEM, BET, and XRD analyses, the structure of carriers was broken to some extent after immobilizing Al-ILs. Catalytic reaction tests show that the SBA-15/Al-ILs composite exhibited the highest catalytic activity among three composite catalysts for the ketalation between cyclohexanone and ethanediol. Under the comparable conditions, the yield (%) of product onto SBA-15/Al-ILs catalyst can reach 85.1%. SBA-15/Al-ILs composite catalyst is a good catalyst for the ketalation between cyclohexanone and ethanediol.

ACKNOWLEDGEMENT

Financial support from Project supported by the National Natural Science Foundation of China (51572115) is gratefully acknowledged.

REFERENCES

1. C. Liao, B. K. Guo, X. G. Sun and S. Dai, *Chem. Sus. Chem.*, **8**, 353 (2015).
2. M. Petkovic, K. R. Seddon, L. P. N. Rebelo and C. S. Pereira, *Chem. Soc. Rev.*, **40**, 1383 (2011).
3. Z. M. Li, Y. Zhou, D. J. Tao, W. Huang, X. S. Chen and Z. Yang, *RSC Adv.*, **4**, 12160 (2014).
4. P. Zhang, T. B. Wu and B. X. Han, *Adv. Mater.*, **26**, 6810 (2014).
5. X. X. Han, W. Yan, C. T. Hung, Y. F. He, P. H. Wu, L. L. Liu, S. J. Huang and S. B. Liu, *Korean J. Chem. Eng.*, **33**, 2063 (2016).
6. S. Xu, C. P. Huang, J. Zhang, J. Liu, X. J. Lao and B. H. Chen, *Korean J. Chem. Eng.*, **26**, 985 (2009).
7. T. Qiu, X. T. Guo, J. B. Yang, L. H. Zhou, L. Li, H. X. Wang and Y. Niu, *Chem. Eng. J.*, **296**, 71 (2016).
8. S. Xu, D. J. Tao, F. F. Chen, Y. Zhou, S. Zhao, L. L. Yu, X. S. Chen and K. Huang, *Korean J. Chem. Eng.*, **33**, 3374 (2016).
9. C. Chiappe and M. Malvaldi, *Phys. Chem. Chem. Phys.*, **12**, 11191 (2010).
10. A. Riisager, R. Fehrmann, M. Haumann and P. Wasserscheid, *Top. Catal.*, **40**, 91 (2006).
11. J. S. Beek, J. C. Vartulli, W. J. Roth, M. E. Leonowicz, C. T. Kresge, K. D. Schmitt, C. T.-W. Chu, D. H. Olson, E. W. Sheppard, S. B. McCullen, J. B. Higgins and J. L. Schlenkert, *J. Am. Chem. Soc.*, **114**, 1083 (1992).
12. A. Pourjavadi, S. H. Hosseini, M. Doulabi, S. M. Fakoorpoor and F. Seidi, *ACS Catal.*, **2**, 1259 (2012).
13. S. Zhang, Q. Zhang and Y. Deng, *Green Chem.*, **13**, 2619 (2011).
14. J. Yang, Y. Hu, L. Jiang, B. Zhou, R. Jia and H. Huang, *Biochem. Eng. J.*, **70**, 46 (2013).
15. M. K. Lee, H. L. Shim, M. M. Dharman, K. H. Kim, S. W. Park and D. W. Park, *Korean J. Chem. Eng.*, **25**, 1004 (2008).
16. Y. Chen and Y. F. Song, *Chem. Plus. Chem.*, **79**, 304 (2014).
17. D. J. Tao, Z. M. Li, Z. Cheng, N. Hu and X. S. *Chen, Ind. Eng. Chem. Res.*, **51**, 16263 (2012).
18. B. R. Jermy and A. Pandurangan, *J. Mol. Catal. A*, **256**, 184 (2006).
19. S. Gadamsetti, N. P. Rajan, G. S. Rao and K. V. R. Chary, *J. Mol. Catal. A*, **410**, 49 (2015).
20. J. N. Armor, *Appl. Catal. A*, **189**, 153 (1999).
21. K. Qiao and Y. Deng, *Mol. Catal. A*, **171**, 81 (2001).
22. H. L. Xin, Q. Wu, M. H. Han, D. Z. Wang and Y. Jin, *Appl. Catal. A*, **292**, 354 (2005).
23. J. Zhang, C. P. Huang, B. H. Chen, P. J. Ren and Z. G. Lei, *Energy Fuels*, **21**, 1724 (2007).
24. Q. Zhao, X. P. Zhou, M. R. Ji, D. L. Wu, T. S. Jiang and H. B. Yin, *Colloids Surf., A*, **384**, 513 (2011).
25. C. Z. Qiao, Y. F. Zhang, J. C. Zhang and C. Y. Li, *Appl. Catal. A.*, **276**, 61 (2004).
26. D. Y. Zhao, J. Y. Sun and Q. Z. Li, *Chem. Mater.*, **12**, 275 (2000).
27. A. Kowalczyk, Z. Piwowarska, D. Macina, P. Kuśtrowski, A. Rokicińska, M. Michalik and L. Chmielarz, *Chem. Eng. J.*, **295**, 167 (2016).
28. C. DeCastro, E. Sauvage, M. H. Valkenberg and W. F. Hölderich, *J. Catal.*, **196**, 86 (2000).
29. M. M. Du, G. W. Zhan, X. Yang, H. X. Wang, W. S. Lin, Y. Zhou, J. Zhu, L. Lin, J. L. Huang, D. H. Sun, L. S. Jia and Q. B. Li, *J. Catal.*, **283**, 192 (2011).
30. C. Cai, H. Wang and J. Y. Han, *Appl. Surf. Sci.*, **257**, 9802 (2011).
31. T. S. Jiang, J. L. Cheng, W. P. Liu, L. Fu, X. P. Zhou, Q, Zhao and H. B. Yin, *J. Solid State Chem.*, **208**, 71 (2014).
32. D. Y. Zhao, Q. S. Huo, J. L. Feng, B. F. Chmelka and G. D. Stucky, *J. Am. Chem. Soc.*, **120**, 6024 (1998).
33. M. Kruk and M. Jaroniec, *Chem. Mater.*, **12**, 1961 (2000).
34. T. S. Jiang, Q. Zhao, M. Li and H. B. Yin, *J. Hazard. Mater.*, **159**, 204 (2008).